Hyperspherical calculations of $H(1s)+\mu^+$ rearrangement collision cross sections from threshold to 2 eV

Z. X. Zhao,[1] A. Igarashi,[2] and C. D. Lin[1]
[1]*Department of Physics, Kansas State University, Manhattan, Kansas 66506-2601*
[2]*Department of Applied Physics, Miyazaki University, Miyazaki, 889-2192, Japan*
(Received 8 May 2000; published 12 September 2000)

Using hyperspherical close-coupling method cross sections for charge-transfer reaction for $H(1s)+\mu^+$ collisions are calculated from threshold up to 2 eV. It is shown that partial-wave cross sections can be obtained using a rotor model which is similar to the standard perturbed stationary-state approximation for ion-atom collisions. The results are compared to $D^+ + H(1s)$ collisions to examine the dependence of transfer cross sections on the masses of the collision partners. Feshbach and some shape resonances are also examined.

PACS number(s): 34.70.+e, 31.15.Ja, 36.10.Dr

I. INTRODUCTION

The charge-transfer process $A^+ + B \rightarrow A + B^+$ is one of the most fundamental reactions in a three-body Coulomb system. Various quantum-mechanical formulations for such reactions have been proposed in the past, and one of the well developed approaches is the hyperspherical close-coupling method [1]. This method has been used extensively for the collisions of electrons or positrons with atomic hydrogen [2–7], and in collisions involving muonic atoms [8]. In these applications the collision system consists of two light particles and a heavy one, or of three particles of nearly equal masses. The hyperspherical method can in principle be applied to prototype ion-atom collisions, consisting of two heavy particles and a light one. In practice the method has never been applied to ion-atom collisions until a very recent publication [9]. For ion-atom collisions, the number of partial waves needed to reach a converged cross section easily runs into hundreds or thousands even for collisions at subthermal energies. In the standard hyperspherical close-coupling approach, each partial wave calculation is done independently, including the calculation of hyperspherical potential curves and coupling terms. Performing such calculations accurately for all the partial waves is an undesirable numerical burden. In the recent article [9], however, two of us have shown that for ion-atom collisions one can perform hyperspherical close-coupling calculations using the rotor model. This model is similar to the standard perturbed stationary-state (PSS) approximation [10] traditionally used for atom-atom and ion-atom collisions where the potential curves and coupling terms only have to be calculated once. Calculations of cross sections for the higher partial waves can be obtained simply by solving the hyperradial equations by adding a centrifugal potential term $J(J+1)/(2\mu\rho^2)$ for each higher partial wave J (μ is the reduced mass and ρ the hyperradius). In [9] the validity of this rotor model is demonstrated for the $D^+ + H(1s) \rightarrow D(1s) + H^+$ collisions. In this paper, we demonstrate the application of the same model to $H(1s)+\mu^+$ rearrangement collisions. By comparing the results with the $D^+ + H(1s)$ collisions it allows us to assess the mass dependence of the reaction cross sections for this class of elementary reactions. We also search for Feshbach resonances below the first excited threshold and some shape resonances.

The only other calculation for this collision system that we are aware of is the work of Matveenko [11]. He started with the PSS model in a two-state approximation. By matching the solutions from the inner region to the correct asymptotic solutions he was able to circumvent the inherent limitations of the PSS model that has an incorrect description of the asymptotic solutions. His results will be compared to ours. In Sec. II we briefly summarize the method used. The main results are presented in Sec. III. A short summary in Sec. IV concludes this report.

II. DESCRIPTION OF THE THEORETICAL METHOD

We use mass-weighted hyperspherical coordinates to describe the three charged particles, μ^+, H^+, and e^-. In the center-of-mass frame, we choose the first Jacobi coordinate $\vec{R}$ to be the vector from μ^+ to H^+, with the reduced mass denoted by μ_1; and the second Jacobi coordinate $\vec{r}$ from the center-of-mass of μ^+ and H^+ to the electron, with the reduced mass μ_2. For this work we define the hyperradius ρ and the hyperangle ϕ by

$$\rho = \sqrt{R^2 + \left(\frac{\mu_2}{\mu_1}\right) r^2}, \tag{1}$$

$$\tan\phi = \sqrt{\frac{\mu_2}{\mu_1}}\frac{r}{R}. \tag{2}$$

Using this definition, the hyperradius ρ is very close to the interparticle separation R between the muon and the proton, and the reduced mass for the motion in ρ is given by μ_1. By treating ρ as the adiabatic parameter, the calculation in hyperspherical coordinates can be carried out in an essentially identical manner to the familiar Born-Oppenheimer approximation where the internuclear separation R is treated as the adiabatic parameter. For each partial wave J, the full Hamiltonian of the collision system is written as [1,6]

$$H = -\frac{1}{2\mu_1}\left(\frac{d^2}{d\rho^2} + \frac{5}{\rho}\frac{d}{d\rho}\right) + h_{ad}(\rho,\Omega) \tag{3}$$

with

$$h_{ad}=\frac{\Lambda^2}{2\mu_1\rho^2}+V(\rho,\Omega), \tag{4}$$

where Λ^2 is the five-dimensional grand angular momentum operator and the variable Ω represents the set of five angles in the hyperspherical space. The Λ^2 operator takes the form

$$\Lambda^2(\Omega)=-\frac{1}{\sin^2\phi\cos^2\phi}\left[\frac{d}{d\phi}(\sin^2\phi\cos^2\phi)\frac{d}{d\phi}\right]+\frac{\vec{\ell}_1^{\,2}}{\cos^2\phi}+\frac{\vec{\ell}_2^{\,2}}{\sin^2\phi}, \tag{5}$$

where $\vec{\ell}_1$ and $\vec{\ell}_2$ are the orbital angular momentum operators for rotational motion associated with each radius vector. The total Coulomb interaction among the pairs of charged particles is represented by V. The adiabatic basis functions are the eigenfunctions of h_{ad}

$$h_{ad}\phi_i=\left(U_i(\rho)-\frac{15}{8\mu_1\rho^2}\right)\phi_i. \tag{6}$$

Substitution of the expansion

$$\Psi=\sum_i \frac{F_i(\rho)}{\rho^{5/2}}\phi_i(\rho;\Omega) \tag{7}$$

into the scattering equation

$$(H-E)\Psi(\rho,\Omega)=0 \tag{8}$$

gives a set of coupled equations

$$\left(-\frac{1}{2\mu_1}\frac{d^2}{d\rho^2}-E\right)F=\left(-U+\frac{1}{2\mu_1}P\frac{d}{d\rho}+\frac{1}{2\mu_1}Q\right)F, \tag{9}$$

where

$$P_{ij}=\left\langle \phi_i\left|\frac{d}{d\rho}\phi_j\right.\right\rangle, \tag{10}$$

$$Q_{ij}=\left\langle \phi_i\left|\frac{d^2}{d\rho^2}\phi_j\right.\right\rangle, \tag{11}$$

$$U_{ij}=\left\langle \phi_i\left|h_{ad}+\frac{15}{8\mu_1\rho^2}\right|\phi_j\right\rangle. \tag{12}$$

Here F is a column vector whose ith component is the function $F_i(\rho)$. Equation (9) is integrated to a large hyperradius $\rho_{\rm end}$ where the solution in hyperspherical coordinates is projected onto the analytical solutions for the dissociated states expressed in Jacobi coordinates. From the projection the reactance matrix K is extracted and the partial wave cross sections are obtained. This matching procedure is detailed in [6,1].

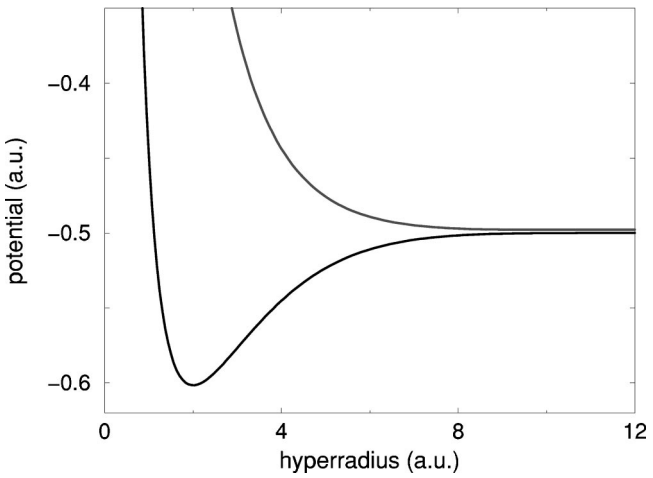

FIG. 1. The lowest two $J=0$ hyperspherical potential curves for the $\mu^+ + \mathrm{H}$ system.

For the present problem, we consider only the two lowest scattering channels. Using atomic units, the mass of the muon is 206.768262, the mass of the proton is 1836.152701, and the mass of the electron is 1.0. The ground states of $\mathrm{H}(1s)$ and of $\mathrm{Mu}(1s)$ are separated by 58 meV, where we use Mu to indicate the bound state of μ^+ and e^-. The first two adiabatic potential curves for $J=0$ are shown in Fig. 1. Since there is no sharped avoided crossing, the present calculations were performed under the standard adiabatic expansion method, including all the nonadiabatic couplings between the two channels. Note that the diabatic-by-sector method which is used for multichannel scattering problems when there are sharped avoided crossings is not used for the present simple situation. The eigenvalues and the eigenfunctions of (6) were obtained by diagonalizing the adiabatic Hamiltonian at each ρ in terms of Sturmian orbitals [6].

III. RESULTS AND DISCUSSION

In Fig. 1 the two lowest $J=0$ potential curves are shown. They resemble the two lowest Born-Oppenheimer potential curves of H_2^+. This is not surprising since the hyperspherical potential curves would reproduce the BO curves of H_2^+ in the limit that the mass of each of the heavy particles goes to infinity. One important difference, however, is in the asymptotic region where the hyperspherical potential curves approach the correct limits of the separated systems, with energies -0.49972784 a.u. for $\mathrm{H}(1s)$ and -0.49759347 a.u. for $\mathrm{Mu}(1s)$. In the BO approach, the two thresholds are degenerate at -0.5 a.u.

To illustrate the asymptotic potential curves in the hyperspherical approach, we show in Fig. 2(a) the lowest two curves for the present system and for later comparison, also the two lowest $J=0$ hyperspherical potential curves for HD^+. In HD^+ the two curves are separated by 3.7 meV asymptotically, with a pronounced avoided crossing near $\rho=12$ a.u. In fact, the nonadiabatic coupling P_{12}, as shown in Fig. 2(b), shows a Lorentz shape with the center at $\rho=11.8$ a.u. For the present $\mu^+ + \mathrm{H}$ system, the larger energy gap in the asymptotic region results in an avoided crossing

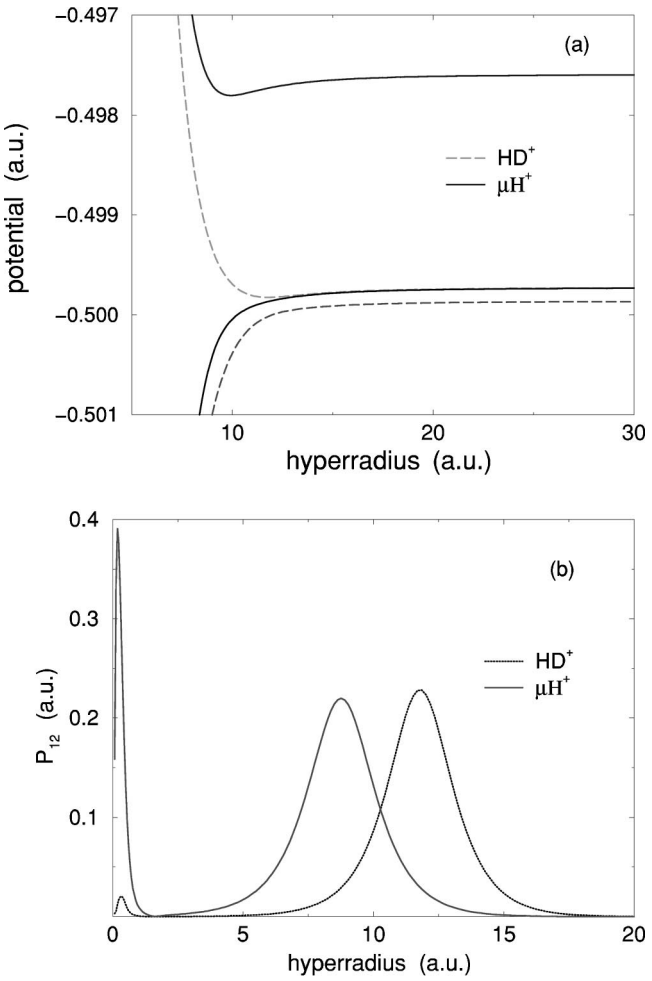

FIG. 2. (a) Comparison of the two lowest $J=0$ hyperspherical potential curves for the $\mu^+ + \mathrm{H}$ system and the HD^+ system at large hyperradial distances. (b) Comparison of the nonadiabatic coupling P_{12} between the two lowest $J=0$ hyperspherical channels for the $\mu^+ + \mathrm{H}$ system and the HD^+ system.

occurring at a smaller hyperradius. In Fig. 2(b) the nonadiabatic coupling shows a Lorentz shape with the peak at $\rho = 7.88$ a.u.

In Fig. 2(a) we note that the second curve for the $\mu^+ + \mathrm{H}$ system has a shallow well at ρ near 8.0. Similar shallow well has been seen for the HD^+ system. Such a shallow well may support Feshbach resonances. We have searched for Feshbach resonances for the present system by solving the coupled equations and found one and only one resonance at -0.3864×10^{-6} a.u. below the Mu(1s) threshold, and the width was calculated to be 2.6×10^{-6} a.u. We are not aware of other calculations for this resonance. (We have searched for Feshbach resonances for other J's but none were found.)

Note that outside the avoided crossing region each pair of potential curves remain very flat. These curves are typical examples showing Demkov coupling [12]. In a semiclassical theory the Demkov coupling predicts transition probabilities that depend sensitively on the ratio E_{12}/v, where E_{12} is the asymptotic energy separation and v is the collision speed. In the present work we are interested in the low energy region where we need to calculate the transition cross section for each partial wave, but the parametrization of the semiclassical theory offers a qualitative interpretation of the results obtained from quantal calculation.

TABLE I. Comparison of partial wave cross sections for $\mu^+ + \mathrm{H}(1s) \rightarrow \mu^+ + \mathrm{H}(1s)$ calculated from the exact hyperspherical approach (bottom line) with those calculated from the rotor model (top line) for $J \neq 0$. Energies are measured from the H(1s) threshold in a.u. and the cross sections are given in atomic units. $A(+B) = A\times10^B$.

E	$J=1$	$J=2$	$J=10$
1.00(−6)	5.4680(+02)	1.4307(+01)	3.1434(−12)
	5.4079(+02)	1.4305(+01)	2.1913(−12)
1.00(−5)	2.9401(+03)	1.6933(+02)	6.2951(−02)
	2.9362(+03)	1.6919(+02)	6.2910(−02)
1.00(−4)	5.7772(+00)	1.0868(+02)	8.0712(−01)
	5.7009(+00)	1.0764(+02)	8.0454(−01)
1.00(−3)	2.7758(−01)	9.9380(+01)	8.6902(+00)
	2.7857(−01)	9.9094(+01)	8.6554(+00)
1.00(−2)	4.3686(+00)	1.5256(+00)	4.0630(+01)
	4.3799(+00)	1.5142(+00)	3.9653(+01)

From the adiabatic potential curves in Fig. 1 and the coupling term in Fig. 2(b), the elastic and charge exchange cross sections for the $J=0$ partial wave are obtained by solving the coupled hyperradial equations (9). In the standard hyperspherical approach, the same procedure has to be carried out for each partial wave. In other words, new hyperspherical potential curves and coupling terms have to be calculated and the resulting coupled hyperradial equations be solved to obtain the scattering cross sections for each J. However, as shown in [9], for a system consisting of two heavy particles and one light one, it is possible to employ the rotor approximation. In this approximation, the potential curves and the coupling terms for each nonzero J do not have to be calculated again. To calculate cross sections for a nonzero J, one needs only to add to each $J=0$ adiabatic potential a centrifugal potential term $J(J+1)/(2\mu_1\rho^2)$ and then solve the resulting hyperradial equations. This approximation is similar to the one employed in the PSS approximation for atom-atom and ion-atom collisions. The PSS approximation, however, has many intrinsic limitations since the equations do not satisfy the correct asymptotic scattering conditions [13]. Using the rotor approximation, the hyperspherical close-coupling calculations can be carried out with the same ease as the PSS approximation but without its intrinsic limitations.

To check the validity of the rotor model for the present system, we compare in Table I some partial wave cross sections carried out using the rotor model and those obtained from the actual hyperspherical calculations. The discrepancies are small except for small partial waves at low energies, such as the comparison at $E=1.0\times10^{-6}$ a.u. for $J=1$. However, at this energy the $J=0$ partial wave has the partial cross section of 3.117×10^4, much larger than the $J=1$ partial wave. Anyway, at such low energies the partial wave convergence is very rapid so a true hyperspherical calculation can be carried out directly.

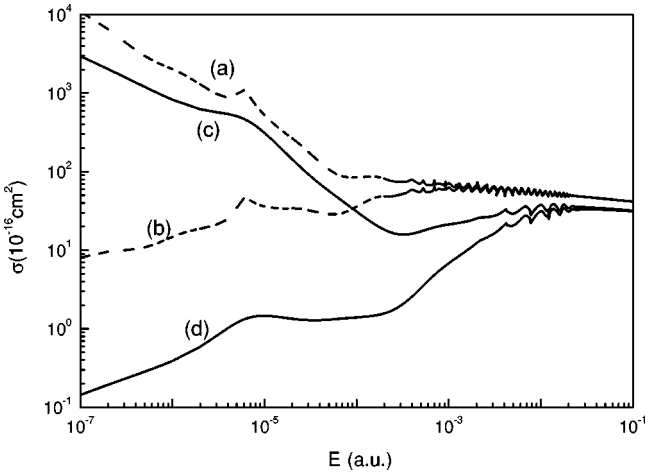

FIG. 3. Comparison of the energy dependence of the total charge exchange cross sections for (a) $D^+ + H(1s) \rightarrow D(1s) + H^+$; (b) $H^+ + D(1s) \rightarrow H(1s) + D^+$; (c) $H^+ + Mu(1s) \rightarrow H(1s) + \mu^+$; and (d) $\mu^+ + H(1s) \rightarrow Mu(1s) + H^+$. The energy is measured from the ground state of the target for each system.

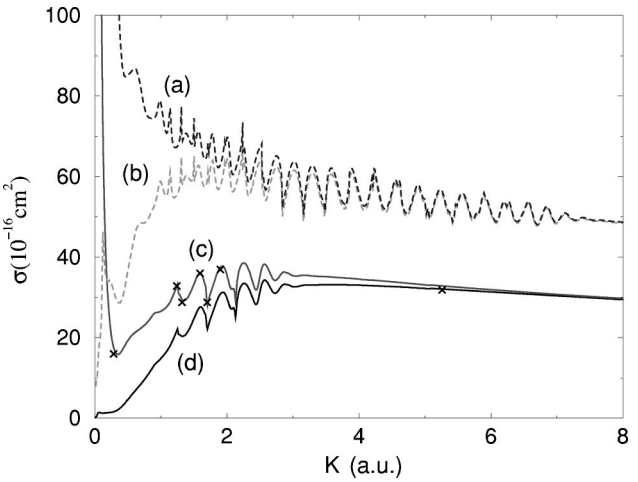

FIG. 4. Same as in Fig. 3 but plotted against the momentum of the incident particle, showing more details in the higher energy region. The crosses are results obtained by Matveenko [11] at selective energy points.

Using the rotor model, we have calculated the $\mu^+ + H(1s) \rightarrow Mu(1s) + H^+$ cross sections from threshold to about 0.1 a.u. in energies. At the highest energy we need about 200 partial waves to achieve good converged rearrangement scattering cross sections. The final results are shown in (d) of Fig. 3. Cross sections for the reverse process, $Mu(1s) + H^+ \rightarrow \mu^+ + H(1s)$, which can be obtained from the principle of detailed balancing, are shown in (c) of Fig. 3. In this figure, we also show the cross section for the $D^+ + H(1s) \rightarrow D(1s) + H^+$ reaction and its time-reversed process, respectively, in (a) and (b). The comparison shows that cross sections near the threshold do indeed depend sensitively on the energy gap in the asymptotic region. We caution that the energy scale is measured from the ground state of the target for each collision.

For the two exothermal reactions, the small energy defect in $D^+ + H(1s) \rightarrow D(1s) + H^+$ results in a much larger cross section near the threshold. The cross section tends to drop with increasing energies, but not without structures. In (a) and (c), in fact, both show a small kink at energies near 6×10^{-6} a.u. This kink was found to be due to the large contribution from the $J=4$ partial wave. Below 10^{-4} a.u. the number of partial waves contributing to the total cross sction is still small and thus the structure of a dominant single partial wave may result in observed structure in the total cross section.

In Fig. 3 several fine oscillating structures in the cross section near 10^{-2} a.u. can be observed. These structures are more clearly displayed in Fig. 4 where the cross sections are shown against the momentum of the incident particle. In (c) we also compare our results from the calculation by Matveenko [11]. In the energy region covered, the two calculations agree quite well. The approximations used by the latter author have no effect on the calculated cross sections at the energies shown, but they may have some effects on the cross sections near the threshold which were not available from [11].

In Fig. 3 the number of oscillations is fewer for $\mu^+ + H(1s) \rightarrow Mu(1s) + H^+$ than for $H^+ + D(1s) \rightarrow H(1s) + D^+$ reactions. Such structures have been seen previously in the PSS-type calculations and are the results of contributions from higher partial waves [14]. They are influenced by the shape resonances from the higher J partial waves, but the peaks cannot be attributed to individual shape resonances.

To understand the origin of these oscillatory structures, in Fig. 5 we display the calculated cross section for $Mu(1s) + H^+ \rightarrow \mu^+ + H(1s)$ and the contributions from the dominant partial waves. We will focus on the origin of the first peak in the total cross section. In the figure, partial wave

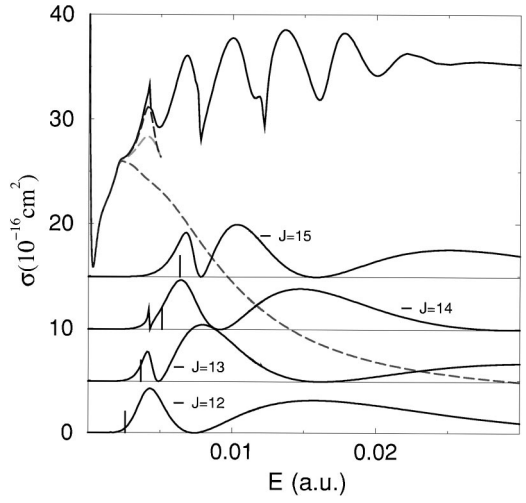

FIG. 5. Analysis of the oscillatory structures of the total cross sections (uppermost solid line) for the $H^+ + Mu(1s) \rightarrow H(1s) + \mu^+$ reaction. The bottom four frames give the partial wave cross sections for $J=12$–15. Each vertical bar indicates the position of the top of the barrier of the effective potential (see text). The lowest dashed lines gives the partial cross sections summed up to $J=12$. The next two dashed lines give the sums up to $J=13$ and $J=14$, respectively.

cross sections for $J=12$, 13, 14, and 15 are shown. For each J, the vertical line indicates the position of the top of the barrier of the effective potential $U(\rho)+J(J+1)/(2\mu_1\rho^2)$, where U is the lowest potential curve of Fig. 1. According to the classical model, orbiting is expected to occur at this energy and contributes to a large classical cross section. In Fig. 5, the lowest dashed lines gives the total partial cross sections summed up to $J=12$. Adding to it the contribution from $J=13$ gives the first indication of the peak, as shown in the second lowest dashed lines. By adding the contribution from the $J=14$ partial wave, shown by the dashed lines right below the total cross section curve, gives the structure which is close to the final result. From the eigenphase shift sum sharp shape resonance like the $J=14$ partial wave has been observed for $J=12$ also. No effort was made to search for the sharp resonances for other partial waves since they are all much narrower than the peaks observed in the total cross section. Based on the relative widths we can state that the narrow shape resonances do not contribute to the peaks.

From Fig. 5, clearly the broad resonance-like structures from $J=12$, 13, 14, and 15 contribute to the first peak even though other partial waves contribute to the ''background.'' Whether we want to identify these broad resonance-like structures as shape resonances is a matter of semantics. All of these broad structures have energies above the potential barriers as indicated by the vertical bars for each partial wave. On the other hand, for each J the nonadiabatic coupling between the two channels can effectively raise the top of the potential barrier of the lower channel when the nonadiabatic effect is included. In this respect at least the first broad peak in each of the $J=12$–15 partial wave may still be viewed as a broad shape resonance. Looking at the partial wave contributions to the peaks in the total cross sections, it is clear that it is not possible to associate each peak to a specific partial wave.

IV. SUMMARY

In summary, we have calculated the rearrangement scattering cross section for the $\mu^+ + \mathrm{H}(1s)$ collision at energies from threshold to 0.1 a.u. using the hyperspherical close coupling method. Using the rotor model we show that the adiabatic potential curves and coupling terms need to be calculated only once, and partial wave cross sections for higher J can be obtained with the same ease as the standard perturbed stationary-state approximation for ion-atom collisions, yet without the inherent limitations of the latter. For collision energies very close to the threshold, however, hyperspherical calculations are still needed but convergence in total cross sections can be achieved by only a few partial waves. Clearly the method can be extended to multichannel collisions.

ACKNOWLEDGMENTS

This work was supported in part by the U.S. Department of Energy, Office of Science, Office of Basic Energy Sciences, Division of Chemical Sciences.

[1] C.D. Lin, Phys. Rep. **257**, 1 (1995).
[2] J.Z. Tang, S. Watanabe, and M. Matsuzawa, Phys. Rev. A **48**, 841 (1993).
[3] Ming-Keh Chen, C.D. Lin, and J.Z. Tang, Phys. Rev. A **56**, 2435 (1997).
[4] Yan Zhou and C.D. Lin, J. Phys. B **28**, 4907 (1995).
[5] Yan Zhou and C.D. Lin, J. Phys. B **27**, 5065 (1994).
[6] A. Igarashi and N. Toshima, Phys. Rev. A **50**, 232 (1994).
[7] A. Igarashi, N. Toshima, and T. Shirai, Phys. Rev. A **50**, 4951 (1994).
[8] A. Igarashi, I. Shimamura, and N. Toshima, Phys. Rev. A **58**, 1166 (1998).
[9] A. Igarashi and C.D. Lin, Phys. Rev. Lett. **83**, 4041 (1999).
[10] B.H. Bransden and M.R.C. McDowell, *Charge Exchange and the Theory of Ion-Atom Collisions* (Oxford, Clarendon, 1992).
[11] A.V. Matveenko, J. Phys. B **10**, 1133 (1977).
[12] Yu. N. Demkov, Zh. Éksp. Teor. Fiz. **45**, 195 (1963) [Sov. Phys. JETP **18**, 138 (1964)].
[13] John B. Delos, Rev. Mod. Phys. **53**, 287 (1981).
[14] N. Shimakura and M. Kimura, Phys. Rev. A **44**, 1659 (1991).